JOURNAL OF GEOPHYSICAL RESEARCH, VOL. 100, NO. C5, PAGES 8777–8790, MAY 15, 1995

Satellite-derived sea surface temperatures: Current status

Ian J. Barton
Division of Atmospheric Research, CSIRO, Aspendale, Victoria, Australia

Abstract. The current status of techniques for deriving sea surface temperatures (SST) from infrared satellite data is reviewed. A short history of the subject is presented, along with a survey of the different techniques employed for obtaining SST from space measurements. The discussion concentrates on the advanced very high resolution radiometer (AVHRR) and similar instruments, as these are found to provide the most useful data for SST estimation. A comparison of different algorithms for deriving SST from the AVHRR instruments shows that there has been little improvement in derivation accuracy over the past decade. The importance of the "first-guess" principle is introduced and shows that some of the more recent "advances" in this field do not address the residual source of error in SST derivation. New algorithms that include coefficients dependent on the variances of the satellite brightness temperature images are found to be difficult to apply to real satellite data. Other new algorithms that include measurements of total atmospheric water vapor column may give a slight improvement in derivation accuracy, but they do not account for anomalous vertical structure in the atmosphere. Directions for future research to improve the accuracy of satellite-derived SST are suggested.

1. Introduction

Sea surface temperature (SST) is now recognized as one of the main controllers and indicators of climate variability. The temperature of the waters in the tropical central and west Pacific Ocean has been linked to the Southern Oscillation Index and the onset and persistence of the El Niño phenomenon [*Cane et al.*, 1966]. The SST regulates the transfer of longwave radiant energy to the atmosphere as well as the latent and sensible heat fluxes into the lower atmosphere.

Early global data sets of SST were generated from ship measurements using bucket and engine intake thermometers, and the accuracy and coverage of these data sets were extremely poor. *Bottomley et al.* [1990] include maps of ship coverage for the three decades 1951-1980 that show no data in the southeast Pacific and the Southern Ocean and limited data in the tropical Pacific. More recently, high-quality measurements from drifting and moored buoys and better quality control of ship data have improved the data sets generated from ground-based measurements, but there are still many data voids in areas not covered by shipping lanes.

Over the last 20 years the use of satellite data to provide global SST data sets has been gradually increasing, and these are now thought to be better than those derived from a combination of conventional in situ measurements. It has been found that the most reliable global data sets of SST are obtained from multichannel infrared radiometers operating in cloud-free conditions. Thus, in producing these data sets, great care must be taken to ensure that the data are not affected by clouds. Before these data sets will be used in climate research and weather forecasting, they need to be more generally available than they have been in the past. The data must be provided with the required spatial resolution and in a timely manner. This is not an easy task and is one that must be addressed before satellite-derived SST data sets gain the confidence of the user community. At the present time a combination of satellite and in situ data provides the most reliable global data sets (see, for example, *Reynolds and Smith* [1994]), but with improved instrumentation and analysis procedures, satellites may provide the bulk of the data used in future SST data sets.

Paper number 95JC00365.
0148-0227/95/95JC-00365$05.00

2. History

Before satellite measurements of SST were available, one of the most widely used SST climatologies was the "Reynolds climatology" [*Reynolds*, 1982] provided by the National Oceanic and Atmospheric Administration/National Environmental Satellite Data and Information Service (NOAA/NESDIS). *Reynolds* [1983] has also undertaken a comparison of six global SST climatologies. More recently, a comprehensive atlas of global SST using in situ data only has been published through the joint efforts of the United Kingdom Meteorological Office and the Massachusetts Institute of Technology [*Bottomley et al.*, 1990]. As well as giving a complete review of the history of SST measurement, this publica-

tion gives an excellent discussion of the various measurement methods, their accuracies, and quality control.

Early work on the use of differential absorption measurements to account for water vapor effects in SST measurement from space was reported by *Anding and Kauth* [1970, 1972] and *Prabhakara et al.* [1974]. These reports were based on the use of data from the infrared interferometer spectrometers carried on the Nimbus 3 and 4 satellites. Later theoretical work by *Deschamps and Phulpin* [1980] investigated the derivation of SST from channels at 3.7, 11, and 12 μm.

One of the first satellite-derived operational products was the GOSSTCOMP product developed by NOAA using early NOAA satellite data [*Brower et al.*, 1976]. The basic instrument was a scanning radiometer with one broad infrared channel and one visible channel. Water vapor correction was derived from the temperature-profiling channels on the vertical temperature profile radiometer, along with data from a single water vapor channel at a wavelength of 18 μm. Cloud clearing was based on histogram techniques using the scanning radiometer data. Accuracies, determined from comparisons with ship and buoy measurements, were around 2 K.

During 1983 and 1984 a series of three workshops was held to compare different methods of deriving SST from satellite instruments [*Njoku*, 1985]. The comparisons showed that in clear sky conditions the infrared techniques were superior to those using microwaves. Although microwaves can "see" through clouds, the accuracy of such a measurement is rather poor (greater than 2 K) and gives no great improvement over using a climatological value. The main errors in the microwave techniques result from surface emissivity variations due to wind speed (temperature is a second-order effect) and water vapor absorption.

A great advance in the measurement of SST was made with the launch of the first AVHRR instrument on the polar orbiting TIROS-N satellite. This first instrument had an extra channel at 3.7 μm and thus allowed for a differential absorption technique to be used to derive a correction for water vapor absorption in the atmosphere. Use of this technique was restricted to nighttime, as the short-wavelength channel included significant reflected solar contribution during the day. Later, five-channel AVHRR instruments on the NOAA meteorological satellites included the so-called "split-window" channels at 10.8 and 11.9 μm, allowing SST determination during the day. Owing to instrument-induced noise limiting the use of the 3.7-μm channel for SST derivation, these two channels have become the workhorse for SST derivation over the last 15 years. Much of the following discussion in this paper relates to the development of new techniques for the analysis of data from these two channels. The discussion also assumes that the data have been accurately screened to ensure that none of the infrared data has been contaminated by clouds.

In the past, geostationary meteorological satellites (Meteosat, GOES, GMS, INSAT) have included a single thermal infrared channel for surface temperature measurement which provides a rough estimate of SST. However, future geostationary satellites will include split-window channels centered near 11 and 12 μm, and thus analysis techniques developed for AVHRR data will be applicable to data from these satellites.

The latest technological advance in the satellite measurement of SST is the recent launch of the along track scanning radiometer (ATSR) on the ERS 1 satellite. This instrument was specifically designed to measure SST and has state-of-the-art calibration techniques and low noise signals on the detectors. An extra advantage is the use of a dual-view scanning system that allows atmospheric correction using two different pathlengths as well as a multiwavelength capability. Global data sets of SST derived from ATSR data are now available to the research community for use in climate applications.

3. Infrared Techniques

3.1 The Basic Algorithm

Infrared radiation leaving the Earth's surface is attenuated by the atmosphere before reaching the satellite instrument. The accurate measurement of SST using infrared radiometers depends on first being able to isolate cloud-free data and then to account for the atmospheric absorption using various techniques. Early single-channel infrared radiometers used climatological data or measurements from other instruments to correct for the atmospheric absorption. This was the limiting factor in the accuracy of the estimation.

With the advent of multiwavelength radiometers using differential absorption techniques, algorithms for deriving SST were developed using brightness temperatures and radiances as inputs. This early work was based on the theoretical work of *McMillin* [1975], who showed that a simple linear combination of the radiances measured at two wavelengths gave a good estimate of the radiance leaving the surface and hence the SST value. Later work by *McMillin and Crosby* [1984] also established a linear relation between the SST and the satellite-measured brightness temperatures, namely,

$$\mathrm{SST} = aT_i + \gamma(T_i - T_j) + c \qquad (1)$$

where T_i and T_j are the brightness temperature measured in channels i and j and c is a constant. In many SST algorithms the coefficient a is assumed to be unity, and in all other algorithms it is close to unity. *McMillin* [1975] also defined the "differential absorption" term γ as

$$\gamma = (1 - \tau_i)/(\tau_i - \tau_j) \qquad (2)$$

where τ is the transmittance through the atmosphere from the surface to the satellite and is given by

$$\tau = exp(-ku) \qquad (3)$$

with k being the mass absorption coefficient of the atmospheric absorbers and u the path length. In cases where there is weak absorption the transmittance can

be approximated by $(1-ku)$ which leads to the expression

$$\gamma \approx (k_i)/(k_j - k_i). \quad (4)$$

Care must be exercised when comparing published values of γ, as *Walton* [1988], *Yu and Barton* [1994], and perhaps others have used a "gamma" that equals $(\gamma+1)$. In this paper the gamma used is that defined in (2), and it is recommended that this definition be used in all future publications. As the values of the absorption coefficients in the atmospheric windows are only weakly dependent on atmospheric parameters, algorithms can be developed that assume a constant value of γ. The basic relation given in (1) remains the backbone of all infrared derivations for SST. Recent techniques, which will be discussed later, include minor nonlinear adjustments, coefficients depending on the angle of measurement, and those where selected extra information has been included. However, the basic linear form of the SST algorithm is evident in all infrared SST algorithms.

3.2 Errors

Pearce et al. [1989] have introduced the noise amplification factor (NAF) which can be used to determine the error introduced into the SST value due to the inherent error (electrical noise and digitization errors) in each of the brightness temperatures. In (1) the NAF is given by

$$\mathrm{NAF} = \sqrt{(a+\gamma)^2 + \gamma^2} \quad (5)$$

and the SST error is then the error in the brightness temperatures (asssumed to be the same for each channel) multiplied by the NAF.

Significant errors in SST values derived from AVHRR data have also occurred in the past owing to the incorrect application of calibration factors and nonlinearity corrections. It is important that when algorithms are published in the future, a clear statement be made on the means to be used to convert from the raw satellite digital counts to brightness temperatures. This has generally not been done in the past and has occasionally led to the incorrect application of AVHRR SST algorithms.

4. AVHRR SST Algorithms

The AVHRR instruments on the NOAA operational meteorological satellites supply global data for deriving SST four times daily. Because the AVHRR data are broadcast from the satellite in real time and a simple S band receiver can be used to receive these data, they are widely used, and many algorithms have been developed for both global and regional applications. For SST estimation the most common algorithms used are those supplied by NOAA called the multichannel MCSST, the "crossed-product" CPSST, and the nonlinear NLSST. This last algorithm is now that used operationally by NOAA (C. Walton, personal communication, 1995). The MCSST is derived from a multiple-regression analysis using coincident satellite and drifting buoy data which gives a linear algorithm with a weak dependence on view angle. A global accuracy of 0.7 K is claimed for this algorithm; this is simply the rms value obtained in the regression analysis used to derive the algorithm coefficients. The MCSST works reasonably well, but some improvements have been noted when a CPSST or an NLSST is used. The CPSST and NLSST have coefficients that are weakly dependent on the magnitude of the brightness temperatures and an estimate of the surface temperature, respectively. The CPSST adjustment was based on a graphical technique which assumed that the atmospheric correction is a function of both the temperature difference in the two channels and the absolute values of the brightness temperatures. Both these algorithms give a "gamma" that is broadly dependent on the surface temperature.

All SST algorithms for AVHRR data have been determined by two basic techniques: either a theoretical atmospheric transmission model with a set of representative vertical profiles of atmospheric temperature and absorbing constituents is used, or a straight regression between coincident satellite brightness temperatures and surface measurements provides the algorithm coefficients. In this latter case, difficulties can arise, as the surface measurements usually give the bulk temperature, while satellites measure the skin temperature. The implications of this difference are discussed in detail by *Wick et al.* [1992].

Because all algorithms have a basic theoretical dependence on the differential absorption technique and they can be reduced to the linear form of the simple algorithm given above, it is possible to extract a value of γ for every algorithm (even though γ can be dependent on latitude, brightness temperature, or some other variable). In those cases when a is not exactly unity, the values of c are adjusted to account for the difference between a and unity. Global algorithms tend to have a close or equal to 1 and a small c, while regional algorithms have a somewhat different to 1 and hence a larger magnitude for c. The parameter c also includes the effects of nonunity surface emissivity, emissivity difference at the two wavelengths, and minor absorbing constituents in the atmosphere, but the contribution by all these effects is quite small.

4.1 Intercomparison of Algorithms

A comparison of selected AVHRR SST algorithms gives a valuable insight into the recent developments in data analysis. For this exercise the following three sets of data were assumed: one each for typical subtropical, midlatitude summer, and midlatitude winter conditions. It is also assumed here that the brightness temperatures to be applied to each algorithm are consistent and are those obtained using the correct calibration coefficients and nonlinearity corrections. The satellite brightness temperatures, water vapor amounts, and the ratio of the variances of the brightness temperatures r [see *Harris and Mason,* 1992] for each set are given in Table 1. These values have simply been selected as typical of the atmospheric conditions. Values of r computed from a relation given by *Sobrino et al.* [1994] are sim-

Table 1. Parameters Selected for the Three Test Atmospheres

	Subtropical	Midlatitude Summer	Midlatitude Winter
W, g/cm^2	3.0	1.5	0.8
T_{11}, K	296.0	287.0	279.0
T_{12}, K	294.5	286.0	278.5
$\Delta T=(T_{11} - T_{12})$, K	1.5	1.0	0.5
r=[Var(T_{12})/Var(T_{11})]	0.8	0.9	0.95
r'	0.788	0.914	0.966

W is the total water vapor column, ΔT is the difference between the two brightness temperatures T_{11} and T_{12}, and r is the ratio of the variances of the brightness temperature in the 12- and 11-μm data. The r' is the ratio of the variances calculated using the relation given by *Sobrino et al.* [1994].

ilar to those selected, giving some confidence that the values assumed in Table 1 are realistic.

The simplest algorithms are those of *Barton* [1983, 1985], *McMillin and Crosby* [1984], *Walton* [1985], and *Sobrino et al.* [1995], which have the coefficient a equal to unity. In these algorithms, γ is between 2 and 3 and c is small. In a second group, a is close to, but not equal to, unity and the value of c depends on the difference between a and unity. Such algorithms have been developed by *McClain* [1983, 1984], *Llewellyn-Jones et al.* [1984], and *Bates and Diaz* [1991].

Other forms of AVHRR algorithms include those by *Harris and Mason* [1992], *Sobrino et al.* [1994], and *Yu and Barton* [1994] which include coefficients that are dependent on the ratio of the variances of the 11- and 12-μm brightness temperatures and those algorithms developed by *Emery et al.* [1994] in their recent work. Note that the value of r used by *Sobrino et al.* [1994] is the reciprocal of that used here and in other papers.

All algorithms referred to above are used to produce values of SST in the nadir for the three selected sets of data, and the results are given in Table 2. Algorithms that have the temperatures input in degrees Celsius instead of Kelvin have had their value of c adjusted accordingly. The results in Table 2 reveal some interesting features. Even though the algorithms have been developed for different AVHRR sensors, different regions, and by theoretical and experimental techniques, there is very good agreement shown by the derived SST values for the three sets of data given in Table 1. This supports the comment made above, that the basic differential absorption algorithm is quite robust and that all the algorithms developed really give the same performance. This does not mean that a single algorithm should be used for all AVHRR instruments but that all the algorithms are similar. Those algorithms that claim to perform better are those developed for particular regions, in which some assumptions are made about the range of atmospheric variability, and the coefficients of the algorithm can then be decreased, resulting in lower noise values for the derived SST. This point is explained in the next section.

4.2 A Graphical Analysis

The simplest multichannel SST algorithm given in (1), with $a = 1$, can be rewritten as

$$D_i = \gamma/(\gamma + 1)D_j + c/(\gamma + 1) \quad (6)$$

where D_i is the difference between the SST value and the satellite-measured brightness temperature T_i. This algorithm can then be shown in graphical form and is done so in Figure 1 for a typical AVHRR value of $\gamma = 2.8$. The slope of the line is $\gamma/(\gamma + 1)$, and the abcissa intercept is $-c/\gamma$. The three cases given in Table 1 are shown on Figure 1.

The more general algorithm in (1) also can be expressed in a similar manner as

$$D_i = \gamma/(\gamma + 1)D_j + c/(\gamma + 1) + xT_i/(\gamma + 1) \quad (7)$$

where $a = 1 + x$. These algorithms have usually been developed with some latitudinal or regional dependence, but they can also be expressed in graphical form. In Figure 2 the algorithm of *Emery et al.* [1994] is shown with a variable γ, and $x = 0.037$. For reference the line from Figure 1 with $\gamma = 2.8$ is also shown in Figure 2. The three dashed lines show the lines with slopes of $\gamma/(\gamma + 1)$ for the three cases given in Tables 1 and 2. The differences between the $\gamma = 2.8$ line and those for *Emery et al.* [1994] are accounted for with the terms $xT_i/(\gamma+1)$ and $c/(\gamma+1)$: for larger values of T_i the point on the dashed line (say, at point A in Figure 2) will move upward (say, to point B) and lie near the original line (generally, larger values of T are associated with larger amounts of atmospheric water vapor and hence larger values of D). For lower values of T_i the opposite is true, and the other end of the line will move downward. Thus these two terms have the effect of tilting the $\gamma/(\gamma + 1)$ line toward that for the simple case in Figure 1. The final algorithm is shown as the solid lines in Figure 2 which are seen to be close to the dotted line representing the simple algorithm in Figure 1. In the cases of *Sobrino et al.* [1994] and the CPSST the adjustments to the $\gamma/(\gamma + 1)$ lines are made through the constant terms which have a dependence on r and the two brightness temperatures, respectively.

In some instances the developers of these regional algorithms claim an improved performance because simulation studies show a lower SST error. This improvement results from a reduced value of γ and hence a lower NAF. However, it is not clear whether these tactics result in an improved real SST retrieval. One way

Table 2. Sea Surface Temperature (SST) Values for the Three Test Atmospheres for Selected Advanced Very High Resolution Radiometer (AVHRR) Algorithms

Algorithm	T/R	a	γ	c	SST (Subtropical)	SST (Midlatitude Summer)	SST (Midlatitude Winter)
			Advanced Very High Resolution Radiometer				
McClain [1983]	R	1.035	3.046	-10.77	300.2	289.3	279.5
Barton [1983]	T	1.000	2.830	-0.07	300.2	289.8	280.3
Llewellyn-Jones et al. [1984]	T	1.056	2.852	-17.18	299.5	-	-
		1.002	1.669	-0.33	-	288.9	280.1
McMillin and Crosby [1984]	R	1.000	2.702	-0.58	299.5	289.1	279.8
McClain [1984]	R	1.021	2.544	-6.07	300.0	289.5	280.1
Walton [1985]	R	1.000	2.490	-0.32	299.4	289.2	279.9
Barton [1985]	T	1.000	2.760	-0.42	299.7	289.3	280.0
Walton [1988], CPSST	R	1.000	1.850	0.57	299.3	-	-
		1.000	1.632	0.53	-	289.2	-
		1.000	1.179	0.44	-	-	280.0
NLSST, NOAA	R	0.906	2.395	27.54	299.4	-	-
		0.906	1.469	27.54	-	289.1	-
		0.906	0.633	27.54	-	-	280.7
Barton et al. [1989]	T	1.010	2.429	-2.07	300.5	290.2	280.9
Minnett [1990]	T	1.002	1.933	-0.32	-	289.2	280.2
Yokoyama and Tanba [1991]	R	1.012	1.913	-2.74	-	289.6	280.6
Sakaida and Kawamura [1992]	R	1.055	1.972	-15.66	-	289.1	279.7
Harris and Mason [1992]	T	1.011	2.085	-2.64	299.7	-	-
		1.011	1.854	-2.64	-	289.3	-
		1.011	1.756	-2.64	-	-	280.2
Bates and Diaz [1991]	R	0.983	2.662	5.20	300.2	290.0	280.8
Emery et al. [1994]	T	1.037	1.634	-9.28	300.0	-	-
		1.037	1.157	-9.28	-	289.4	-
		1.037	0.935	-9.28	-	-	280.4
Sobrino et al. [1995]	T	1.000	2.520	0.14	299.9	289.7	280.4
Sobrino et al. [1994]	T	1.000	2.716	-0.64	299.4	-	-
		1.000	2.397	-0.06	-	289.3	-
		1.000	2.262	0.19	-	-	280.3
Yu and Barton [1994]	T	1.000	2.122	0	299.2	-	-
		1.000	3.229	0	-	290.2	-
		1.000	4.112	0	-	-	281.1
AVHRR average SST value					299.8	289.4	280.3
AVHRR standard deviation					0.39	0.38	0.42
			Along-Track Scanning Radiometer				
Barton et al. [1989]	T	0.996	2.672	1.50	300.3	290.0	280.7
Závody et al. [1994]	T	1.040	2.898	-12.13	300.1	-	-
		1.007	2.658	-1.90	-	289.8	280.4
Sobrino et al. [1995]	T	1.000	2.710	-0.05	300.0	289.7	280.3

T and R indicate whether the algorithm was derived from theoretical studies of transmission through the atmosphere or from a regression analysis with satellite and surface measurements. Values of the coefficient a, the differential absorption term γ and the constant c are also given. CPSST is the crossed-product sea surface temperature algorithm, and NLSST is the nonlinear sea surface temperature algorithm, both supplied by the National Oceanic and Atmospheric Administration.

of looking at these algorithms is to consider how the correction for the atmospheric absorption is applied.

In the case of the algorithms with $a = 1$ the correction applied to the value of T_i is directly proportional to the difference in the brightness temperatures: this is the true differential absorption technique. In cases where a is slightly larger than unity the algorithm can be written as

$$D_i = xT_i + \gamma(T_i - T_j) + c \quad (8)$$

and there are two components to the correction for absorption D_i: again, one part is directly proportional to the difference in the brightness temperatures, while the second part is proportional to the value of T_i. This latter component is just a "single-channel" correction term. Therefore these algorithms that have a reduced value of γ are combinations of one-channel and two-channel algorithms. Given that single-channel algorithms perform poorly (hence the necessity to use two channels) and that the differential absorption is a direct measure of the correction required, it is not immediately clear that these "improved" algorithms in fact give a better measure of SST in spite of having lower values of γ and thus lower NAF values.

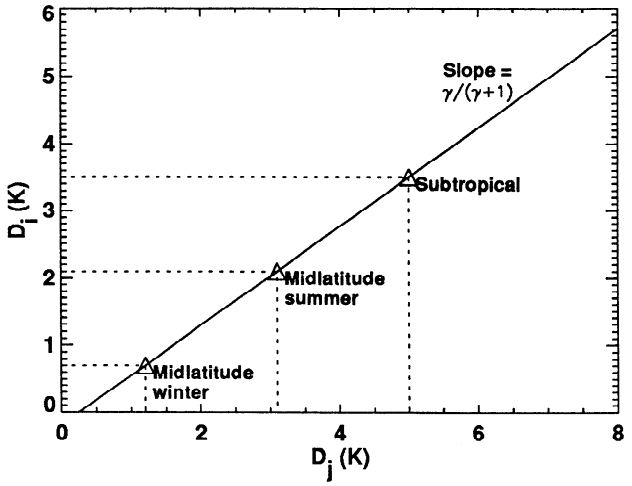

Figure 1. A graphical representation of the simple sea surface temperature (SST) algorithm SST=T_i + $\gamma(T_i - T_j) + c$. Here D_i=SST-T_i, the slope of the line is $\gamma/(\gamma+1)$, and the abcissa intercept is $-c/\gamma$. The three situations given in Table 1 are displayed.

In these algorithms, γ has become more a measure of how much differential absorption information to include in the SST estimate rather than a direct measure of the effect of water vapor absorption. Thus a large value of γ may only be useful if there are low-noise brightness temperatures available. In cases where the satellite data are noisy an algorithm with a lower value of γ may be more appropriate. In the limit, one could reduce γ to zero and have a low NAF and hence a low error in (simulated) SST, but then we are back to using a single channel for SST retrieval.

These analyses indicate the importance of having low-noise data in the derivation of SST from satellite data. Such data are now being supplied by the ATSR instrument on the ERS 1 satellite, and the algorithms used with these data are described in the next section.

5. The ATSR Instrument

The ATSR operational SST algorithms were developed at the Rutherford Appleton Laboratory before launch using a line-by-line transmission model and a set of radiosonde data supplied by the United Kingdom Meteorological Office. Even with the extra information provided by the six "channels" of the ATSR (three wavelengths for two different path lengths), the basic operational algorithms are still a linear combination of a selection of brightness temperatures. The algorithms are given by *Závody et al.* [1994]. Four different algorithms were developed and, depending on data availability, are implemented in the following heirarchy (here 12, 11, and 3.7 refer to the approximate central wavelength and N and F refer to the nadir and forward views): SST1 is where all six channels are used (12N, 11N, 3.7N, 12F, 11F, 3.7F); SST2 includes three nadir channels (12N, 11N, 3.7N); SST3 includes 11- and 12-μm nadir and forward (12N, 11N, 12F, 11F); and SST4 includes 11- and 12-μm nadir only (12N, 11N).

For each algorithm and for each of three regions (tropical, midlatitude, and polar), *Závody et al.* [1994] supply five sets of coefficients for the bands 0-50, 50-100, 100-150, 150-200, and 200-256 km away from the subsatellite track. A blend of these algorithms is used as follows, depending on the latitude of the observation: 0° to 12.5°, tropical algorithm used; 12.5° to 37.5°, interpolate between tropical and midlatitude; 37.5° to 62.5°, interpolate between midlatitude and polar; and 62.5° to 90°, polar algorithm used.

Other ATSR algorithms have been developed by *Barton et al.* [1989] and *Sobrino et al.* [1995]. The ATSR algorithms using the 11- and 12-μm nadir view data have also been applied to the data sets of Table 1, and the resulting SST values appear at the bottom of Table 2. As with the AVHRR algorithms, there is only a small variance shown by the results.

The conical scanning mechanism of the ATSR limits the swath width to 500 km which is considerably narrower than the swath of the AVHRR. However, this is not a major concern, as the ATSR was designed primarily to supply data for climate applications. Detailed intercomparisons between ATSR and AVHRR data have been reported by *Mutlow et al.* [1994] and *Barton et al.* [1995].

6. Image Variance Techniques

The concept of using the variance in the brightness temperature images to determine atmospheric and surface parameters has been introduced by *Kleespies and McMillin* [1990] and *Jedlovec* [1990] to estimate surface temperature and precipitable water amounts from both satellite and airborne multichannel radiometers. This technique has been expanded by *Harris and Mason* [1992] to allow determination of SST algorithm coefficients using the ratio of the variances in the split-window channels. Assuming that the atmosphere is horizontally homogeneous over a specified area and any variation in the brightness temperature image is solely

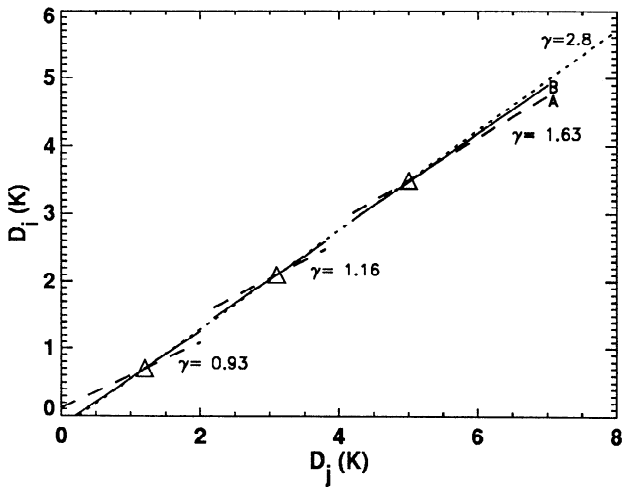

Figure 2. A graphical representation of the SST algorithm SST=$aT_i + \gamma(T_i - T_j) + c$. A full description is given in the text.

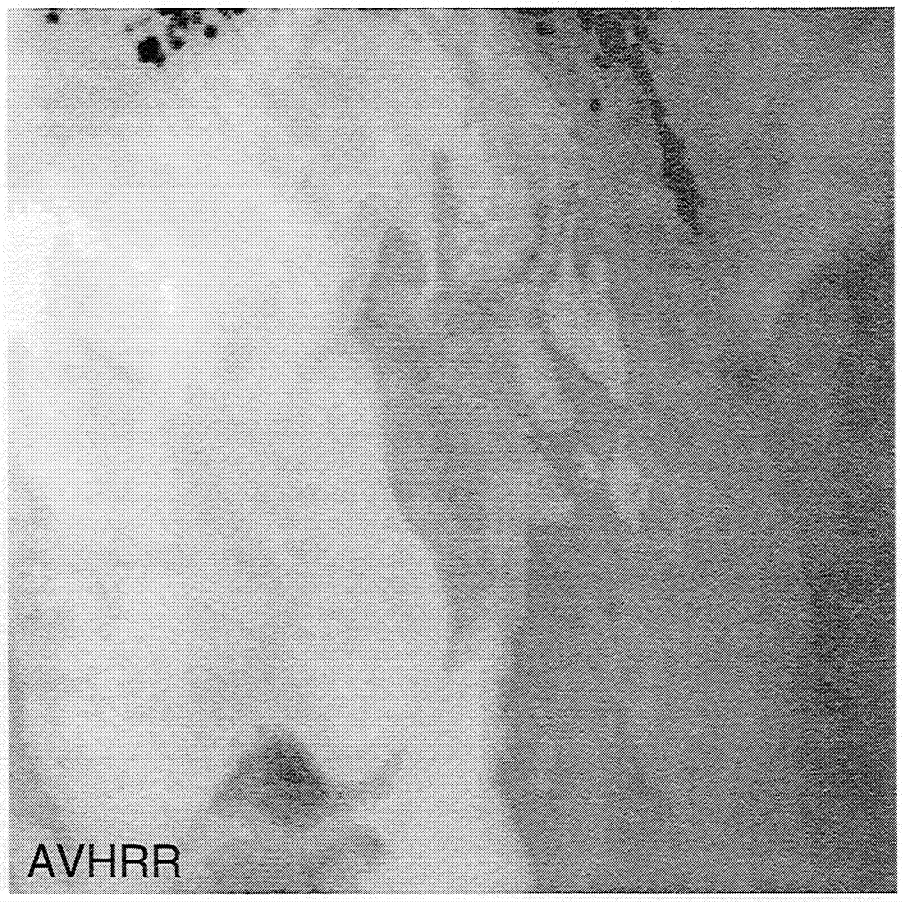

Figure 3. An image of 11-μm brightness temperatures obtained by the advanced very high resolution radiometer (AVHRR) on the NOAA 11 satellite. The image consists of 200 x 200 pixels, was obtained at 1636 UT on September 1, 1991, and is centered near 24°S, 156°E.

due to variations in the SST field, a simple theoretical analysis shows that the ratio of the variation (standard deviation) in the 12- and 11- μm channels, r, can be given as

$$r = \frac{\sigma_{12}}{\sigma_{11}} = \frac{\varepsilon_{12}\tau_{12}}{\varepsilon_{11}\tau_{11}}. \quad (9)$$

σ_i, ε_i, and τ_i are the standard deviation of the brightness temperature data, the surface emissivity and the transmittance from the surface to space for channel i, respectively. Algorithms developed using this technique have shown a marked improvement in derived SST accuracy when applied to simulated data. *Yu and Barton* [1994] and *Sobrino et al.* [1994] have developed similar theoretical algorithms, but in the latter case the surface emissivity is assumed to be unity and the ratio is simply that of the two transmittances from the surface to space.

Yu and Barton [1994] indicated that the variance techniques rely on the ability to derive a stable value for the value of the ratio. They suggested that the 10-bit digitization of the AVHRR data may limit the usefulness of this technique but that ATSR data with its 12-bit resolution may provide accurate SST values using variance techniques. To investigate this further, two sets of data have been analyzed, one from from the AVHRR instrument on the NOAA 11 satellite and the second from the ATSR. The two images are at the same location and were received on consecutive days in September 1991. The 11-μm images from each instrument are shown in Figures 3 and 4. Similar patterns in the brightness temperature can be identified in the bottom left corner of the images. The small amount of cloud in the top of the AVHRR image does not affect the subsequent data analysis. For different areas in the images the value of r has been calculated by three different techniques as follows: (1) The r_1 is derived using the method suggested by *Yu and Barton* [1994] in which the ratio is determined by a selective statistical method, as

$$r_1 = \sum_S \left[\frac{T_{12}(n) - \overline{T_{12}}}{T_{11}(n) - \overline{T_{11}}}\right] / N \quad (10)$$

where the selection S is $D/2 \leq | T_{11}(n) - \overline{T_{11}} | \leq 2D$, D is the variance in the 11-μm image, and N is the number of pixels in the chosen area that are used to form the ratio. This selection ensures that the ratio does not include those cases where $T_{11}(n)$-$\overline{T_{11}}$ is close to zero. (2) The r_2 is the average value of the ratio $[T_{12}(\mathrm{n})\text{-}\overline{T_{12}}]/[T_{11}(\mathrm{n})\text{-}\overline{T_{11}}]$. (3) The r_3 is simply the ratio of the variances in the two channels.

The results are presented in Table 3. The pixel/line origin is in the bottom left corner of Figures 3 and 4,

Figure 4. An image of 11-μm brightness temperatures obtained by the along-track scanning radiometer (ATSR) on the ERS-1 satellite. The image consists of 200 x 200 pixels, was obtained at 1223 UT on September 2, 1991, and is centered near 24°S, 155°E.

and the "pixels" column gives the number of pixels used in the derivation of r_1. Theoretically, it is expected that the values of r would lie between 0.8 and 0.95 and perhaps be close to 0.9. Also, given that the atmosphere is assumed to be homogeneous, at least over the selected areas, the values of r in adjacent areas should be similar. However, there does not appear to be any consistency in the values; indeed, in many cases the values of r are greater than unity. The large range of values for r_2 also shows the importance of not including cases where $T_{11}(n)$-$\overline{T_{11}}$ is close to zero. The negative values arise from cases where $T_{11}(n)$ is greater than the mean value while $T_{12}(n)$ is smaller than its mean, or vice versa.

The lack of consistency for the values of r indicates that the derivation of the ratio is quite unstable and that these "ratio" methods are difficult to apply on an operational basis. This is true for both the AVHRR and the ATSR data. Histograms of the distribution of the differences between the brightness temperatures and their mean values show the effect of digitization of the satellite data (see Figures 5, 6, 7 and 8). When the ratio r is determined by taking the ratio of these differences for each pixel, the result is a spread of values due to the discrete digitization levels of the data. Figures 9 and 10 show the distribution of the ratio values for individual pixels in a 20 by 20 selected area.

Table 3 shows that although the variance methods work on simulated satellite data, they experience difficulties when applied to real satellite data. Even with the low-noise, 12-bit data from the ATSR, the derivations of the ratio using variances in the brightness temperature images are quite unstable. Table 3 also shows that there is no improvement in the situation if the size of the selected area is varied or if the brightness temperatures are spatially averaged. Of course, much care must be taken with averaging, as the "signal" of the variation in brightness temperature images may be removed if the data are averaged over too large an area.

The failure of these variance techniques may be due to a combination of the following two factors: (1) the basic assumption of a uniform atmosphere overlying an ocean surface with variable SST may be wrong (i.e., the SST is more uniform than the overlying atmosphere) and (2) the data digitization effects may dominate the analysis.

7. Latest Developments

Many researchers are looking for new analysis techniques to improve the quality of geophysical products derived from satellite data. For the SST these attempts have fallen into four broad groups. The variance tech-

Table 3. Values of the Ratios of the Standard Deviations (r_1, r_2 and r_3) in the 11- and 12-μm Brightness Temperature (T_{11} and T_{12}) Images for Selected Areas in the ATSR and AVHRR Data.

Instrument	Area	Origin	Pixels	r_1	r_2	r_3	$\overline{T_{11}}$	$\overline{T_{12}}$	Standard Deviation T_{11}	Standard Deviation T_{12}
ATSR	20x20	0,0	292	0.983	0.951	1.066	292.57	291.23	0.286	0.304
		20,0	209	0.858	0.994	1.020	292.15	290.86	0.144	0.147
		0,20	134	1.016	1.078	1.137	293.11	291.80	0.126	0.143
		20,20	230	0.925	0.817	0.955	292.72	291.47	0.283	0.271
		70,20*	279	0.884	0.904	0.913	292.23	291.01	0.554	0.506
AVHRR	20x20	0,0	221	0.887	0.857	0.963	292.68	291.50	0.185	0.178
		20,0	215	1.054	0.984	1.077	292.77	291.50	0.223	0.240
		0,20	309	0.948	0.911	0.958	292.82	291.68	0.347	0.332
		20,20	225	1.238	1.252	1.298	293.03	291.82	0.126	0.163
		60,20*	310	0.952	1.138	0.982	291.97	290.86	0.496	0.487
ATSR	50x50	0,0	1912	0.980	0.839	0.992	292.69	291.41	0.447	0.443
		50,0	1825	0.925	0.924	0.931	292.42	291.19	0.465	0.433
		0,50	1744	1.088	-0.178	1.267	293.27	292.02	0.101	0.128
		50,50	1692	0.919	1.013	1.177	292.96	291.74	0.105	0.124
AVHRR	50x50	0,0	1745	0.985	0.947	1.042	292.77	291.56	0.327	0.341
		50,0	2046	1.032	1.046	1.035	292.16	291.03	0.352	0.364
		0,50	1878	0.913	-92.477	1.110	293.20	292.09	0.231	0.257
		50,50	1159	0.983	0.982	0.975	292.53	291.48	0.282	0.275
ATSR	100x100	0,0	6235	0.969	0.959	0.987	292.83	291.59	0.456	0.451
		100,0	6304	0.636	0.739	0.907	292.89	291.81	0.207	0.188
		0,100	4588	1.156	1.687	1.224	293.36	292.24	0.210	0.257
		100,100	7017	0.918	0.865	0.980	293.13	292.21	0.337	0.330
AVHRR	100x100	0,0	5713	0.971	0.998	1.006	292.67	291.54	0.485	0.488
		100,0	6007	1.088	1.091	1.079	290.94	289.82	0.687	0.742
		0,100	6393	1.085	1.209	1.132	293.00	291.99	0.631	0.714
		100,100	5290	1.096	1.137	1.109	291.06	289.92	0.723	0.802
ATSR†	20x20	0,0	298	0.981	0.932	1.003	292.57	291.23	0.268	0.269
		20,0	230	0.958	1.062	1.021	292.15	290.86	0.130	0.133
AVHRR†	20x20	0,0	237	0.870	1.015	0.946	292.68	291.50	0.166	0.157
		20,0	218	1.045	1.198	1.055	292.77	291.50	0.218	0.230
ATSR†	50x50	0,0	1902	0.976	1.120	0.983	292.69	291.41	0.438	0.430
		0,50	1549	1.193	1.164	1.257	293.27	292.02	0.088	0.111
AVHRR†	50x50	0,0	1559	1.000	1.161	1.036	292.77	291.56	0.317	0.328
		0,50	1337	1.037	0.161	1.101	293.20	292.09	0.222	0.245
ATSR†	100x100	0,0	6171	0.971	1.193	0.982	292.83	291.59	0.448	0.440
		100,0	6232	0.638	-0.107	0.865	292.89	291.81	0.195	0.169
AVHRR†	100x100	0,0	5767	0.973	0.863	1.003	292.67	291.54	0.477	0.479
		100,0	6241	1.085	1.108	1.078	290.94	289.82	0.685	0.739

Overbars indicate averages.
* Selected area covers the SST front evident in Figures 3 and 4.
†Brightness temperature images have been smoothed by a 5 by 5 pixel filter.

niques have been discussed in section 6; the other three are each discussed in the following sections.

7.1 Inclusion of Water Vapor

As the water vapor content in the atmospheric path increases, the basic assumptions underlying the principles of a linear SST algorithm become less valid, and adjustments to the algorithm coefficients are required. *Emery et al.* [1994] have expanded the approximation underlying the linear algorithm to a second-order term and thus derive a theoretical algorithm that includes a term that is dependent on the total water vapor content. They use a regression analysis on simulated data to derive algorithm coefficients. These new algorithms show some improvement against the CPSST and MCSST products at high latitudes but, surpris-

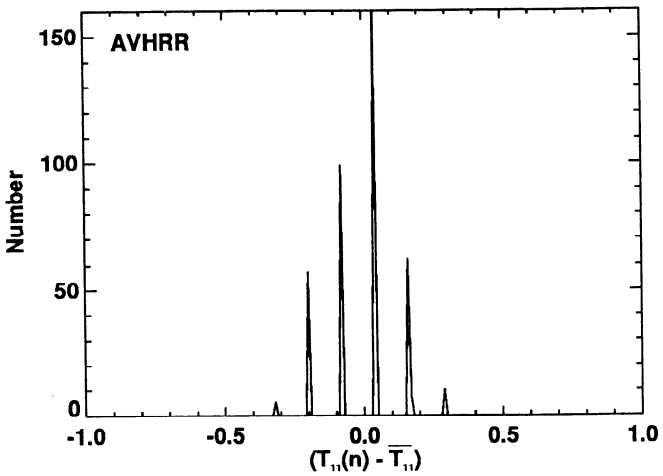

Figure 5. The distribution of the brightness temperatures in the 11-μm AVHRR image about their mean value. The area selected is 20 x 20 pixels with an origin at (20,20).

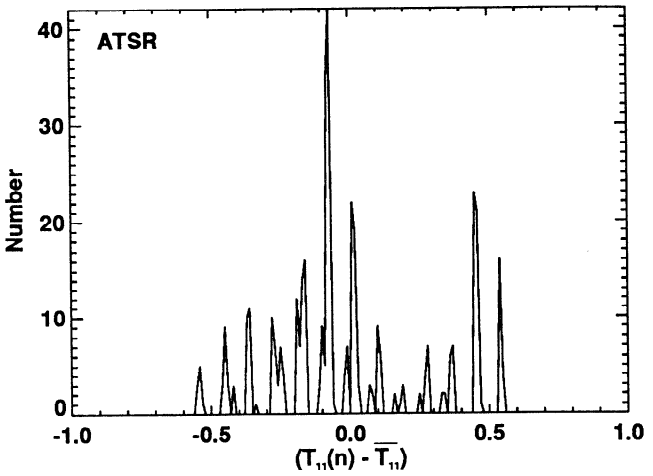

Figure 7. The distribution of the brightness temperatures in the 11-μm ATSR image about their mean value. The area selected is 20 x 20 pixels with an origin at (20,20).

ingly, show no improvement at midlatitudes. In their validation study they use the total water vapor content, as derived from the special sensor microwave imager (SSMI) instruments on the DMSP satellites, in a linear term. When applying these data, they use 2-day averages of water vapor content combined with the infrared data from the AVHRR. The use of such algorithms will present difficulties, given that the data come from two different satellite systems with different orbit characteristics.

Sobrino et al. [1994], in their study using simulated data, derive an algorithm that has coefficients dependent on the ratio of the variances in the 11- and 12-μm images. However, they take their analysis one step further and derive a relation between r and the water vapor content W. In essence, when a measure of W is available, their algorithm coefficients can depend solely on water vapor amount. The authors show that there will be some improvement in derived SST using simulated data but suggest that accurate values of W will be required to gain a significant improvement.

Simulation studies undertaken by *Barton et al.* [1989] have shown that there is only a small benefit in including water vapor information if the noise on the infrared measurements is low. Thus, for ATSR data, there appears to be little benefit in including total water vapor content in the algorithms, unless the water vapor can be determined from satellite data far more accurately than is currently possible.

Steyn-Ross et al. [1993] report a new technique that uses an iterative procedure with a standard water vapor profile and claim an improved SST accuracy. In areas where water vapor profile information is not available this procedure uses the standard shape of the profile as a first guess, and thus the results should not show a significant improvement over those derived using other regional algorithms.

7.2 Latitude or Temperature Dependence

Many of the algorithms included in Table 2 have coefficients that depend on latitude, location, or brightness temperature, and these often give a small improvement

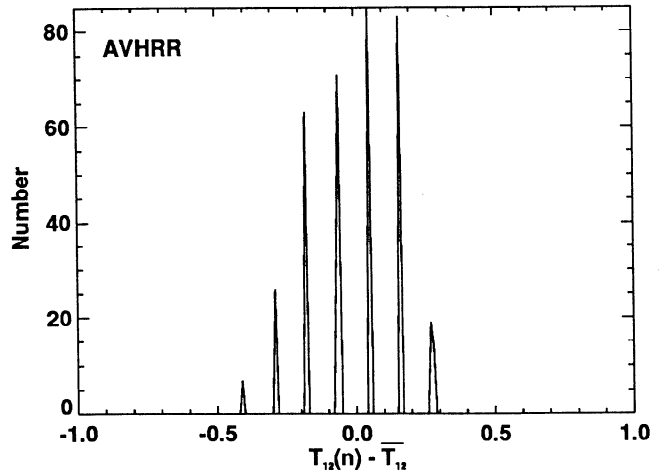

Figure 6. Same as Figure 5, but in the 12-μm AVHRR image.

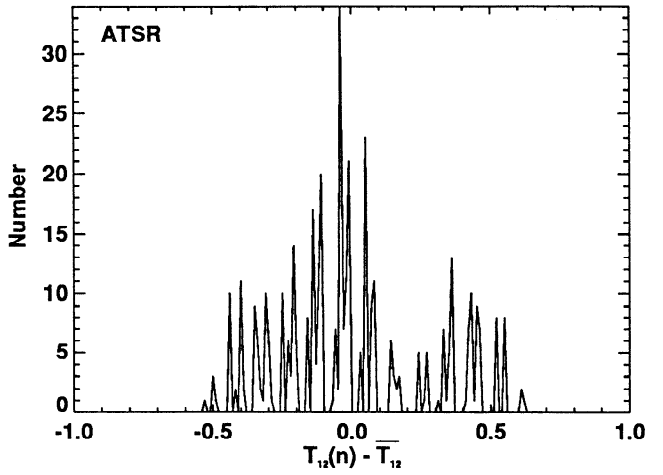

Figure 8. Same as Figure 7, but in the 12-μm ATSR image.

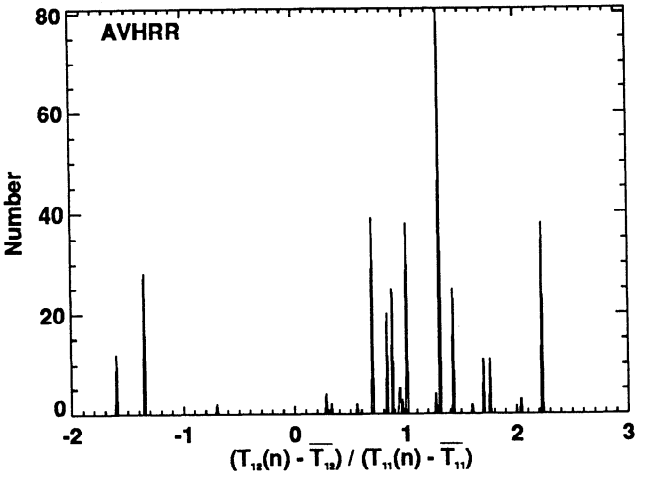

Figure 9. The distribution of the ratio $[T_{12}(n) - \overline{T_{12}}]/[T_{11}(n) - \overline{T_{11}}]$ for the AVHRR image area selected in Figures 5 and 6.

over global algorithms. For example, the CPSST algorithm has coefficients that are dependent on the values of the brightness temperatures, while the ATSR uses different algorithms, depending on the latitude of the scene. Included in this category are those algorithms derived for a particular location or climate. In some ways these algorithms are similar to those dependent on water vapor amount. The basic assumption is that as latitude decreases, the brightness temperature increases and the total water vapor content of the atmosphere also increases.

7.3 Nonlinear Algorithms

Although *McMillin* [1975] suggested that a nonlinear regression algorithm gave a significant improvement over linear methods, no further algorithms of this kind have been reported until the recent work of *Emery et al.* [1994]. Their algorithms have terms that include the difference in the brightness temperatures in the 11- and 12-μm channels as well as the square of the difference in the brightness temperatures. *Emery et al.* [1994] find that when this is done, the SST retrieval accuracy is similar to that from their algorithm that uses the total water vapor content. The improved performance of this form of algorithm has also been independently confirmed by the author and A. Závody (personal communication, 1993).

8. "First-Guess" Principles

Algorithms for deriving SST from satellite data, whether obtained from theoretical transmission models or from a direct regression analysis of coincident satellite and ground-based data, assume a "first guess" of the state of the atmosphere in their application. This general concept has been discussed by *Rodgers* [1976] and, more recently, by *Eyre* [1987] in the context of deriving vertical temperature profiles from TIROS operational vertical sounder (TOVS) data. In the case where a set of radiosonde profiles has been used to derive an algorithm the first guess is simply the average value of the profiles used. A corollary of this principle is if the state of the atmosphere is identical to the first guess, then a perfect retrieval will be made when the algorithm is applied to the data.

In the case of SST algorithms the first guess would be a "typical shape" of the vertical profiles of water vapor and temperature. Deviations from this first guess could then, in most cases, be expected to give errors in the derived SST value. However, there will still be situations where abnormalities at different levels or different structure in the temperature and water vapor profiles will offset each other, and a good retrieval will be made. In other words, all SST algorithms will give perfect retrievals as long as the atmospheric state is equivalent to their first guess. Therefore the secret of a good algorithm is for it to be representative of the state of the atmosphere in the region for which the algorithm is to be applied. Thus the first guess for global algorithms should represent the average state of the atmosphere over the world's oceans, and the success of such algorithms depends on the variance of the "average state".

Having established the importance of the first guess in SST algorithms, it is evident that errors in the derived SST occur when the state of the atmosphere is different to that of the first guess. Therefore attempts to improve the quality of SST retrieval should address the problem of either modifying the first guess or detecting those situations where the atmospheric state is different from the first guess.

9. The Way Forward

9.1 Technological developments

Early results from the ATSR instrument show the advantages of improving instrument technology in deriving accurate SST values [*Mutlow et al.*, 1994, *Barton et al.*, 1995]. Brightness temperatures can be obtained with less noise by improving detector performance through decreasing detector temperatures and

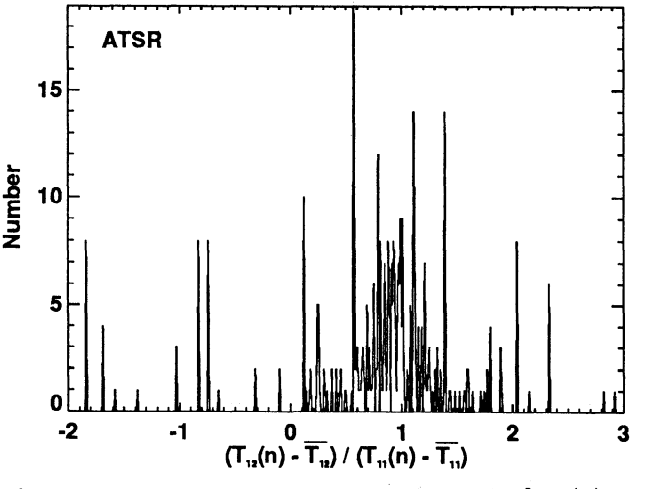

Figure 10. The distribution of the ratio $[T_{12}(n) - \overline{T_{12}}]/[T_{11}(n) - \overline{T_{11}}]$ for the ATSR image area selected in Figures 7 and 8.

other means. When this is done, it is also important to decrease digitization noise by providing 12-bit data as well as to improve absolute calibration by providing more accurate and stable onboard calibration targets. These three improvements must all occur together since if one is absent, the advantages provided by the other two are severely diminished.

One other capability of the ATSR is the multiangle measurements provided by its conical scan mirror. This has the following two advantages: first, the derivation of SST in areas with significant aerosol contamination appears to be improved [*Závody et al.*, 1994], and second, the three extra measurements of brightness temperature should enable the detection of anomalous atmospheric structure and the subsequent application of selective SST algorithms.

A major improvement for AVHRR instruments would be the provision of a 3.7-μm channel with low noise. Because this channel is least affected by water vapor variations, it would allow an improved estimate of SST during the night. The presence of the third useful channel may also provide a means for detecting anomalous vertical structure in the atmosphere. Future satellite instruments that are to be used for SST determination should incorporate extra channels to assess the state of the atmosphere. Such channels can be incorporated into the same instrument (as with the moderate-resolution imaging spectrometer (MODIS)) or be part of another instrument on the same satellite (e.g., the ocean color and temperature scanner (OCTS) and the interferometric monitor for greenhouse gases (IMG) on the ADEOS platform).

9.2 Improved Analysis Procedures

NASA and NOAA, in their joint Pathfinder program, have made valuable advances in the recalibration of the AVHRR infrared channels as well as the application of the nonlinearity corrections. These advances have allowed the development of a long-term global data set of SST from the AVHRR instruments. However, there are still a multitude of algorithms developed by researchers around the world for their particular area of interest and application. In most cases these algorithms have been tested against surface data and suit the needs of the researchers; it is only in the derivation of global data sets that more advanced algorithms are required.

Further efforts should be made to develop operational algorithms that include a term using the square of the difference in brightness temperatures. This was suggested 20 years ago by *McMillin* [1975] and, until recently, seems to have been completely neglected.

Much recent effort has been applied to the development of regional algorithms and variance techniques, but the analyses presented in this paper suggest that these "advances" in algorithm development are not providing the improved accuracy required for climate applications of the data sets. All the algorithms developed for the AVHRR 11- and 12-μm channels have been found to be rather similar, the differences only being in the region of application or some other independent variable (water vapor, latitude, etc.). These algorithms would give a comparable error if an anomalous water vapor profile was present in the atmosphere. This is due to the same basic structure of the algorithms and their inability to include extra information about water vapor structure. The algorithms using the ratio of the brightness temperature variances do not appear to be operationally feasible, and the use of total water vapor contents, where they are available with some reliability, does not appear to provide a greatly improved product.

The way forward seems to be enveloped in the basics of the first-guess principle. Algorithms which depend either on a variable first guess or on deviations from the first-guess state of the atmosphere need to be developed. In the case of SST estimation this implies that some extra information is required on abnormalities in the vertical profiles of water vapor and temperature.

For AVHRR data there are now two ways to apply this concept. First, one can develop algorithms for different states of the atmosphere depending on local climate, but this will not account for deviations from the assumed first guess in each particular location. Second, one can assume that the extra information will be held in the relative values of the brightness temperatures in the three infrared channels and develop a strategy for using this information. This does not mean simply developing a three-channel algorithm, as this just retreats to another first guess. The three brightness temperatures must be used to develop a knowledge of water vapor or temperature structure in the atmosphere, and then the information used to modify the first guess.

For ATSR these principles become more obvious as the six infrared brightness temperatures can in fact be considered as sounding channels for water vapor in the lower troposphere. Then subtle variations in the brightness temperature differences can be attributed to water vapor and temperature structure. A preliminary simulation study investigating this possible application of ATSR data has been described by *Barton et al.* [1994]. Because the ATSR instrument includes two passive microwave channels that provide a nadir measure of total water vapor column [*Eymard et al.*, 1994], it is possible to use this measurement as a constraint in the retrieval of water vapor vertical distribution.

The new iterative technique developed by *Steyn-Ross et al.* [1993] may be one method that could lead to an improved SST derivation. They adjust a standard water vapor profile and look for agreement between the satellite-measured brightness temperatures and those computed using LOWTRAN. Presently, the water vapor profiles are adjusted by using a constant factor at all levels, but if the adjustment was able to be made from a knowledge of the vertical distribution of water vapor, then great improvements in accuracy could be expected.

Future satellite instruments, such as MODIS on the NASA EOS platform, will provide data in many infrared channels which can be used to derive SST in the manner described above. Meanwhile, techniques need to be developed which refine the SST derivation so that departures from the first-guess state of the atmosphere can be taken into account.

Acknowledgments. José Sobrino has provided an advance copy of the paper referred to as *Sobrino et al.* [1995], and the opportunity to include discussion on this paper is appreciated. Charlie Walton (NOAA) and Doug May (U.S. Naval Research Laboratory) have supplied details of the NLSST algorithms. The author also thanks two anonymous reviewers who have suggested some valuable additions to the original manuscript.

References

Anding, D., and R. Kauth, Estimation of sea surface temperature from space, *Remote Sens. Environ., 1,* 217-220, 1970.

Anding, D., and R. Kauth, Reply to the comment by G.A. Maul and M. Sidran, *Remote Sens. Environ., 2,* 171-173, 1972.

Barton, I.J., Dual channel satellite measurements of sea surface temperature, *Q. J. R. Meteorol. Soc., 109,* 365-378, 1983.

Barton, I.J., Transmission model and ground-truth investigation of satellite-derived sea surface temperatures, *J. Clim. Appl. Meteorol., 24,* 508-516, 1985.

Barton, I.J., A.M. Závody, D.M. O'Brien, D.R. Cutten, R.W. Saunders, and D.T. Llewellyn-Jones, Theoretical algorithms for satellite-derived sea surface temperatures, *J. Geophys. Res., 94,* 3365-3375, 1989.

Barton, I.J., A.M. Závody, C.T. Mutlow, and D.T. Llewellyn-Jones, Water vapour retrievals using combined ATSR infrared and microwave data, in Proceedings of the Second ERS-1 Symposium, Space at the Service of our Environment, *Eur. Space Agency Spec. Publ. ESA SP-361,* 819-824, 1994.

Barton, I.J., A.J. Prata, and R.P. Cechet, Validation of the ATSR in Australian waters, *J. Atmos. Oceanic Technol., 12,* 290-300, 1995.

Bates, J.J., and H.F. Diaz, Evaluation of multi-channel sea surface temperature product quality for climate monitoring, *J. Geophys. Res., 96,* 20,613-20,622, 1991.

Bottomley, M., C. K. Folland, J. Hsiung, R.E. Newell, and D.E. Parker, *Global Ocean Surface Temperature Atlas,* MIT Press,Cambridge, Mass., 1990.

Brower, R.L., H.S. Gohrband, W.G. Pichel, T.L. Signore, and C.C. Walton, Satellite derived sea-surface temperatures from NOAA spacecraft, NOAA Tech. Memo. *NESS 78,* 73 pp., 1976.

Cane, M.A., S.E. Zebiak, and S.C. Dolan, Experimental forecasts of the El Nino, *Nature, 321,* 827-832, 1986.

Deschamps, P.Y., and T. Phulpin, Atmospheric correction of infrared measurements of sea surface temperature using channels at 3.7, 11 and 12 μm, *Boundary Layer Meteorol., 18,* 131-143, 1980.

Emery, W.J., Y. Yu, G.A. Wick, P. Schluessel, and R.W. Reynolds, Correcting infrared satellite estimates of sea surface temperature for atmospheric water vapor attenuation, *J. Geophys. Res., 99,* 5219-5236, 1994.

Eymard, L., A. Le Cornec, and L. Tabary, The ERS-1 microwave radiometer, *Int. J. Remote Sens., 15,* 845-857, 1994.

Eyre, J.R., On systematic errors in satellite sounding products and their climatological mean values, *Q. J. R. Meteorol. Soc., 113,* 279-292, 1987.

Harris, A.R., and I.M. Mason, An extension to the split-window technique giving improved atmospheric correction and total water vapour, *Int. J. Remote Sens., 13,* 881-892, 1992.

Jedlovec, G.J., Precipitable water estimation from high-resolution split window radiance measurements, *J. Appl. Meteorol., 29,* 863-877, 1990.

Kleespies, T.J., and L.M. McMillin, Retrieval of precipitable water from observations in the split window over varying surface temperatures, *J. Appl. Meteorol., 29,* 851-862, 1990.

Llewellyn-Jones, D.T., P.J. Minnett, R.W. Saunders, and A.M. Závody, Satellite multichannel infrared measurements of sea surface temperature of the NE Atlantic Ocean using AVHRR/2, *Q. J. R. Meteorol. Soc., 110,* 613-631, 1984.

McClain, E.P., NOAA satellite-derived operational sea surface temperature products, Proceedings of the Satellite-Derived Sea Surface Temperature: Workshop-I, *JPL Publ. 83-34,* appendix C, 16 pp., 1983.

McClain, E.P., Multi-channel sea surface temperatures from the AVHRR on NOAA-7, Proceedings of the Satellite-Derived Sea Surface Temperature: Workshop-II, *JPL Publ. 84-5,* 1-8, 1984.

McMillin, L.M., Estimation of sea surface temperatures from two infrared window measurements with different absorption, *J. Geophys. Res., 80,* 5113-5117, 1975.

McMillin, L.M., and D.S. Crosby, Theory and validation of the multiple window sea surface temperature technique, *J. Geophys. Res., 89,* 3655-3661, 1984.

Minnett, P., The regional optimization of infrared measurements of sea surface temperature from space, *J. Geophys. Res., 95,* 13,497-13,510, 1990.

Mutlow, C.T., A.M. Závody, I.J. Barton, and D.T. Llewellyn-Jones, Sea surface temperature measurements by the along-track scanning radiometer (ATSR) on the ERS 1 satellite: Early results, *J. Geophys. Res., 99,* 22,575-22,588, 1994.

Njoku, E.G., Satellite-derived sea surface temperature: Workshop comparisons, *Bull. Am. Meteorol. Soc., 66,* 274-281, 1985.

Pearce, A.F., A.J. Prata, and C.R. Manning, Comparison of NOAA/AVHRR-2 sea surface temperatures with surface measurements in coastal waters, *Int. J. Remote Sens., 10,* 37-52, 1989.

Prabhakara, C., G. Dalu, and V.G. Kunde, Estimation of sea surface temperature from remote sensing in the 11- to 13-μm window region, *J. Geophys. Res., 79,* 5039-5044, 1974.

Reynolds, R.W., A monthly averaged climatology of sea surface temperatures, *NOAA Tech. Ref. NWS31,* 35 pp., 1982.

Reynolds, R.W., A comparison of sea surface temperature climatologies, *J. Clim. Appl. Meteorol., 22,* 447-459, 1983.

Reynolds, R.W., and T.M. Smith, Improved global sea surface temperature analyses using optimum interpolation, *J. Clim., 7,* 929-948, 1994.

Rodgers, C.D., Retrieval of atmospheric temperature and composition from remote measurements of thermal radiation, *Rev. Geophys., 14,* 609-624, 1976.

Sakaida, F., and H. Kawamura, Estimation of sea surface temperatures around Japan using the Advanced Very High Resolution Radiometer (AVHRR)/NOAA-11, *J. Oceanogr., 48,* 179-192, 1992.

Sobrino, J.A., Z.-L. Li, and M.P. Stoll, Impact of the atmospheric transmittance and total water vapor content in the algorithms for estimating satellite sea surface temperatures, *IEEE Trans. Geosci. Remote Sens., 31,* 946-952, 1994.

Sobrino, J.A, Z.-L. Li, M.P. Stoll and F. Becker, Multi-channel and multi-angle algorithms for estimating sea and land surface temperature with ATSR data, *Int. J. Remote Sens.,* in press, 1995.

Steyn-Ross, M.L., D.A. Steyn-Ross, P.J. Smith, J.D. Shepherd, J. Reid, and P. Tildesley, Water-vapor correction method for advanced very high resolution radiometer data, *J. Geophys. Res., 98,* 22,817-22,826, 1993.

Walton, C.C., Satellite measurement of sea surface temperature in the presence of volcanic aerosols, *J. Clim. Appl. Meteorol., 24,* 501-507, 1985.

Walton, C.C., Nonlinear multichannel algorithms for estimating sea surface temperature with AVHRR satellite data, *J. Appl. Meteorol., 27,* 115-124, 1988.

Wick, G.A., W.J. Emery, and P. Schluessel, A comprehensive comparison between satellite-measured skin and multichannel sea surface temperature, *J. Geophys. Res., 97,* 5569-5595, 1992.

Yokoyama, R., and S. Tanba, Estimation of sea surface temperature via AVHRR of NOAA-9 - Comparison with fixed buoy data, *Int. J. Remote Sens., 12,* 2513-2528, 1991.

Yu, Y., and I.J. Barton, A non-regression-coefficients method of sea surface temperature retrieval from space, *Int. J. Remote Sens., 15,* 1189-1206, 1994.

Závody, A.M., M.R. Gorman, D.J. Lee, D. Eccles, C.T. Mutlow, and D.T. Llewellyn-Jones, The ATSR data processing scheme developed for the EODC, *Int. J. Remote Sens., 15,* 827-843, 1994.

I. J. Barton, Division of Atmospheric Research, CSIRO Marine Laboratories, P. O. Box 1538, Hobart, Tasmania 7001, Australia. e-mail: ijb@ml.csiro.au.

(Received July 28, 1994; revised January 31, 1995; accepted January 31, 1995.)